2023 IEEE Symposium on Electromagnetic Compatibility & Signal/Power Integrity (EMC+SIPI) | 979-8-3503-0976-8/23/$31.00 ©2023 IEEE | DOI: 10.1109/EMCSIPI50001.2023.10241568

On Finding an Equivalent Force to Mimic the Multilayer Ceramic Capacitor Vibration

Yifan Ding[1], Jianmin Zhang[2], Mingfeng Xue[3], Shengyin Ding[4], Benjamin Leung[5], Eric A. MacIntosh[6], Chulsoon Hwang[7]
EMC Laboratory, Missouri University of Science and Technology, Rolla, MO-65401, USA
dingyif@mst.edu[1], hwangc@mst.edu[7]
Google Inc., USA
jianmin@google.com[2], mingfengx@google.com[3], shengyinding@google.com[4], benleung@google.com[5], ericmac@google.com[6]

***Abstract*—The multilayer ceramic capacitor (MLCC) can vibrate due to the piezoelectric effect when there is AC noise on the power rail. The vibration of the capacitor will generate a force on the PCB and thus cause the PCB vibration and audible problems may occur. The work in this paper finds an equivalent force with similar behavior to the MLCC-generated force. The force is controllable and knowable and thus can mimic the capacitor vibration on the PCB.**

Keywords—Multilayer ceramic capacitor, piezoelectric effect, PCB vibration, modal analysis, harmonic analysis, laser Doppler vibrometer (LDV), vibration generated force

I. Introduction

The increasing operation speed requirement of electrical circuits brings the analog and digital communication system grows more complex. To ensure the system behaves stable while remaining functional, low-impedance power distribution network (PDN) is required to control the voltage ripple [1]. Decoupling capacitors are used to efficiently lower the PDN input impedance in the frequency range typically from a few hundred kilohertz to one- or two-hundred megahertz [2] with the resonance zeros formed by the capacitance and serial inductance. Multilayer ceramic capacitor (MLCC) is a typical decoupling capacitor type used in the PDN design. While performing the function of stabilizing the system, it can cause other issues as well.

When there is noise existing in the power rail, it can cause the MLCC to vibrate due to the piezoelectric effect of the dielectric inside the capacitor [3]. The vibration of the capacitor will lead to a vibration of the PCB as shown in Fig. 1, and if the frequency of the noise is in the audible range it will produce acoustic noise. The noise is especially obvious in electronic products like earbuds. In the power delivery path from the source to destination, if too much energy is dissipated as mechanical energy of vibration when passing through MLCC, it will also have a negative impact on the power integrity of the system.

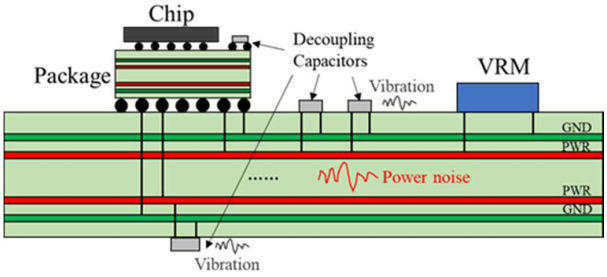

Fig. 1. PDN power rail noise caused electrical component vibration

There are some studies about MLCC vibration behavior from the acoustic noise perspective. For the simulation, there is a simulation methodology for the acoustic noise induced by the MLCC given in [4]. A more detailed and practical simulation flow for MLCC-based acoustic noise analysis is provided in [5]. For the measurement, a measurement methodology for the MLCC-induced acoustic noise is shown in [6]. Another methodology to detect capacitors generating audible acoustic noise in PDN of mobile systems by observing the AC voltage droop on MLCC is given in [7]. Furthermore, the relationship between the characteristics of the acoustic noise and the dynamic characteristics of the PCB are analyzed and the correlation between the acoustic noise and MLCC vibration is given in [8].

There is also a crucial link in the process from the capacitor vibration to the acoustic noise generation. While the capacitor is soldered on the PCB and vibrating, a force will be applied to the PCB at the contact surface between the MLCC and the soldering pad. The complete process is a transformation from the electrical level to the mechanical level, and finally to the sound level. If the force generated by the MLCC can be known, it would be helpful for the system behavior prediction and optimization.

There are some studies about the force applied to the PCB. The work in [9] adopts the capacitance sensing scheme for its high sensitivity for the shear force sensor. But it requires an additional manufacturing process for the PCB. For the force related to MLCC, in [10] the development and normalization of a novel sensor system built with low-cost industrial-grade MLCC is given. But it requires an additional circuit. The study for the pattern of the capacitor vibration generated force is at the beginning stage. The measurement and simulation would be challenging. From practical experience, the capacitor's vibration-generated force could be affected by many factors, such as the supply voltage level, the soldering condition, and some others that are unknown. Finding an equivalent and controllable force to mimic the cap vibration behavior and study its effect on the PCB system is the exact motivation behind this work.

The paper is organized as follows. The PCB vibration mechanism and analysis are given in Section II to demonstrate how an external force applied to the PCB will affect the system behavior. In Section III, an application example is introduced to find an equivalent force of the MLCC vibration-generated force. The results in Section IV show the reliability of the equivalent force that can be measured, controlled, and used for prediction. Conclusions are finally given in Section V.

II. PCB Vibration Analysis

Lorentz Force between a magnet and a coil carrying current will be first discussed in this section. Then, the PCB vibration mechanism analysis will be given to provide the theory support for solving the problem.

A. Lorentz Force on a Current-Carrying Wire

Some assumptions about the MLCC vibration-generated force are given here. Firstly, due to the piezoelectric effect of

the MLCC dielectric, the force it induces on the board is changing direction following the supply voltage change. Secondly, the force is out of the plane of the PCB. Thirdly, the MLCC vibration-generated force is small, and when it is leading the PCB to vibrate the system should be still in the linear region. The equivalent force should have the same characteristics as the force induced by the MLCC described above. Furthermore, the equivalent force should also have the same effect on the PCB as the MLCC force, such as the PCB vibration velocity and vibration pattern at the same frequency.

The force from a coil-magnet system can meet the above requirements. When a current-carrying wire is placed within a magnetic field, each of the moving charges experiences the Lorentz Force. Incorporating the Lorentz Force Law into a non-moving wire yields the following equation in the integral form:

$$F = I \int dl \times B \tag{1}$$

where I is the current on the wire, and B and F are time-harmonic magnetic flux density and force, respectively.

B. PCB Vibration with External Force

The general equation of motion is given in (2). The total force applied to the system $\{F(t)\}$can be decomposed to three terms: the first term $[M]\{\ddot{u}\}$represents the force for inertia $F_{inertia}$, the second term $[C]\{\dot{u}\}$ represents the force for damping $F_{damping}$, and the third term $[K]\{u\}$ is for the force for stiffness $F_{stiffness}$.

$$[M]\{\ddot{u}\} + [C]\{\dot{u}\} + [K]\{u\} = \{F(t)\} \tag{2}$$

where,

$[M]$ is the structural mass matrix

$[C]$ is the structural damping matrix

$[K]$ is the structural stiffness matrix

$\{F\}$ is the load vector

$\{\ddot{u}\}$ is the nodal acceleration vector

$\{\dot{u}\}$ is the nodal velocity vector

$\{u\}$ is the nodal displacement vector

(t) is the time

The physical connection between the PCB vibration and the externally applied force is represented by the above equation of motion. After applying the external force, with the mass, damping, and stiffness of the system, the acceleration, velocity, and displacement response can be then obtained. In the engineering process, the mass, damping, and stiffness information can be obtained from the design, and the acceleration, velocity, and displacement can be obtained by the laser doppler vibrometer (LDV).

The forces with the same amplitude and loading angle from different sources at the same location will have the same effect on the PCB vibration, and the forces are independent of the PCB system. By comparing the PCB vibration patterns and responses, it can show whether the loaded forces to the system are the same. This makes it possible to find an equivalent force to mimic the capacitor vibration behavior.

C. Damping Ratio

The damping ratio is a dimensionless measure describing how oscillations in a system decay after a disturbance and is related to the structural damping matrix $[C]$ presented in (2). In actual vibration, because of the existence of friction, the energy initially obtained by the vibration system will perform negatively on the system due to the resistance. It is necessary to consider the damping ratio to correctly mimic the vibration of the system.

Many methods can be used to calculate the damping ratio. The half-power method in (3) is one of the approaches used for estimating damping based on finding the bandwidth of each mode.

$$\gamma = \frac{\Delta\omega}{2\omega_r} \tag{3}$$

where,

$\Delta\omega$ is the normalized bandwidth of the resonant response at the amplitude of $0.707v_{max}$

ω_r is the resonance frequency.

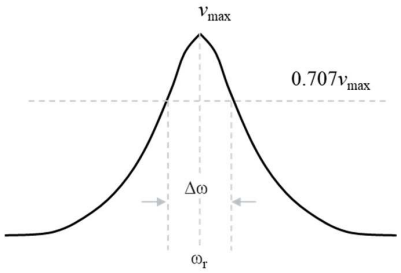

Fig. 2. Half power method for damping ratio calculation

III. Application Example

The application for the PCB vibration observation is a 4-layer board with different power planes. Several capacitor soldering pads are placed to load the external force at different places. Four holes in the middle and four holes near the edges can be fixed with the screws. The size of the board is 39.56mm * 56.56mm.

A. Measurement Setup

The overview of the measurement setup is shown in Fig. 3. The LDV is used to measure the motion of the PCB when there is an external force applied to the system and causing the system vibration. There is a control computer that has a graphical user interface to give input and show the measured results. Also, it can control the laser control module which has the function of laser positioning and power signal input. The DUT is placed under the laser head and on the isolation table within the range that can be irradiated by the laser point. The isolation table is used to eliminate the effect on the measurement from the vibrations out of the system. When an out-of-system vibration source is transmitted to the tabletop, the honeycomb structure and damping of the tabletop can effectively reduce the vibration deformation of the optical table. In addition to supporting, the main function of the vibration isolation legs is to isolate the vibration from the ground.

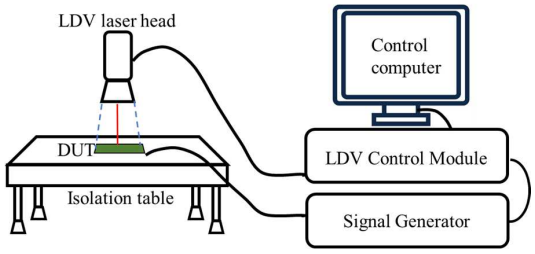

Fig. 3. Overview of the measurement setup

The external force applied to the PCB in this example is generated by the coil-magnet system introduced in Section II. The location to apply the external force is at the corner of the board because of the limitation of coil size and screws. A capacitor soldered on the board provides a stronger connection between the magnet and the PCB. However, there will be no electrical input to the capacitor, so the PCB is in the open loop condition and there will be no force from the capacitor piezoelectric effect in the system. The magnet is attached to the cap top surface using glue. The magnet is very small and very lightweight so the impact of its additional mass on the board vibration can be ignored. The coil is put right under the magnet and its center is aligned with the magnet to minimize stretch in the horizontal direction to the PCB. The boundary condition applied to this setup is 2 fixed points. The board is fixed using two screws at two locations – the left top and right bottom corner shown in Fig. 4(a) - by applying a proper force to screws to ensure the PCB will not move and deformed during the measurement process. In this example, the AC input current to the coil is 2mA as a constant for all the frequencies.

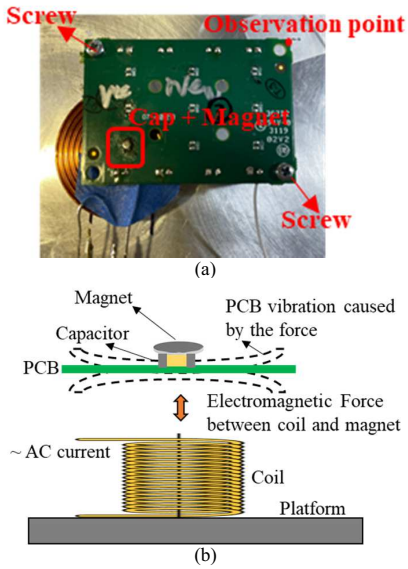

Fig. 4. PCB with the electrical source of the mechanical force. (a) top view of the real setup, showing the location of applied force, the boundary condition (fixed screws) and the observation point. (b) Schematic of the coil-magnet system and the impact to the PCB.

In the measurement, 20 averages are used to minimize the run-to-run variation. The frequency resolution is set to be 0.25Hz to achieve good accuracy.

At different frequencies, the board vibration can be small in certain locations. Therefore, the observation point location is carefully selected to ensure a good accuracy of board vibration responses in the measurement. Because the PCB has larger vibration at its self-resonance frequency, it is reasonable to focus on the frequency range close to the board resonance frequency. Fig. 4(a) shows the location of the observation point, board fixed point, and cap/magnet where the external force from the coil-magnet system is applied to the board. Note that the observation point is selected diagonally towards the magnet near the edge and away from the two fixed screws. This location has a large board vibration velocity at some mode frequencies.

B. *Simulation Setup*

2 separate simulations are required in this study: 1) the coil-magnet force simulation and 2) the PCB vibration simulation.

1) Coil-Magnet simulation model

To obtain the force generated by the coil and magnet, a simulation model is built in Ansys Maxwell 2D based on the geometry of the real setup as shown in Fig. 5. The model is built for half of the cross-section in the x-z plane through the center. The z-axis represented the center of the coil-magnet system, which aligns the centers of the magnet and the coil. In the simulation, a constant current in 2 mA is input to the coil from the cross-section in all the turns as what was done in the measurement.

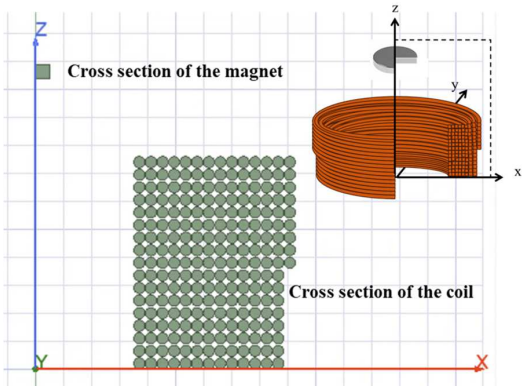

Fig. 5. Ansys Maxwell 2D simulation model for coil-magnet force extraction

2) PCB vibration simulation model

The simulation model for the PCB vibration simulation is built in Ansys Mechanical. The PCB model is based on the design file. The details of the stack-up information including the material in each layer and the layer thickness are given in Fig. 6(a). The signal layers are a mixture of copper and resin, with traces, pads, planes, and the dielectric in the cut-off region. The complicated layer layout requires a huge amount of mesh and will make it quite time-consuming for the simulation. To simplify the design, the signal layers are regarded as solid planes with the materials formed by the copper-dielectric mixture in different ratios to account for different layouts. The material properties such as the layer mass density (unit g/cm^3), coefficient of thermal expansion (CTE_{xy} for in-plane and CTE_z for out-of-plane, unit 10^{-6}/°C), and Young's modulus (E_{xy} for in-plane and E_z for out-of-plane, unit MPa) are given in Fig. 6(b). Correctly setting the material properties are necessary to ensure the PCB resonance mode frequency and pattern match the real situation.

Layer	Type	Material	Thickness
1	SIGNAL	COPPER (78.5%) / COPPER-RESIN	50.8 µm
2	Laminate	Generic FR-4	138.18 µm
3	SIGNAL	COPPER (82.8%) / COPPER-RESIN	30.5 µm
4	Laminate	Generic FR-4	304.8 µm
5	SIGNAL	COPPER (80.2%) / COPPER-RESIN	30.5 µm
6	Laminate	Generic FR-4	138.18 µm
7	SIGNAL	COPPER (84.1%) / COPPER-RESIN	50.8 µm

(a)

Layer	Density	CTExy	CTEz	Exy	Ez
1	7.3735	24.566	24.566	89,458	89,458
2	1.9000	17.000	70.000	24,804	3,450
3	7.6788	23.173	23.173	94,166	94,166
4	1.9000	17.000	70.000	24,804	3,450
5	7.4942	24.015	24.015	91,319	91,319
6	1.9000	17.000	70.000	24,804	3,450
7	7.7711	22.752	22.752	95,590	95,590

(b)

Fig. 6. Details about (a) PCB stack-up material and thickness. (b) PCB layer properties

The fixed boundary conditions in the simulation are defined by the circles with the same radius and locations as the screws applied in the measurement, as shown in Fig. 7. Similarly, the observation point is positioned using the imprinted shapes at the mesh nodes.

After obtaining the simulated force from the coil-magnet system using Maxwell 2D, the force will be applied to the location of the cap at the contact surface between the capacitor bottom and the board to mimic the force in measurement to see the response results.

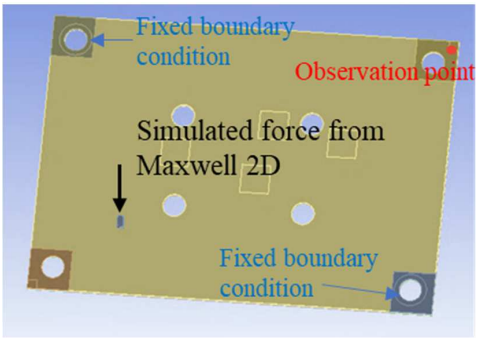

Fig. 7. Ansys Mechanical simulation model for PCB vibration response

IV. Results Analysis

The coil-magnet simulation in Maxwell 2D is done first. In the frequency range of interest (20Hz-20kHz), the simulated force is around 2.4uN with the 2mA input current.

For the PCB vibration simulation, TABLE I compares the 1st mode resonance frequency between the simulation and measurement. The results are correlated very well with a difference of 0.59%.

TABLE I. PCB 1ST Self-Resonance Frequency (Hz) Comparison for 2-fixed Points Boundary Condition

Mode	Measurement	Simulation	Δ
1	390.25	387.93	0.59%

Then, the damping ratio for the selected observation point is extracted using (3) and the result is shown in Fig. 8. The damping ratios will be used in the simulation process in Ansys Mechanical to accurately mimic the system response after a force vector is applied. The simulated vibration response will have a big discrepancy when applying or not applying the damping ratio, as shown in Fig. 9.

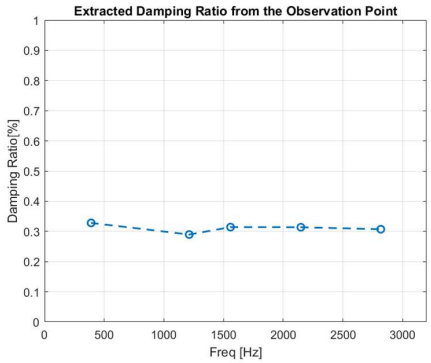

Fig. 8. PCB damping ratio extracted from the observation point

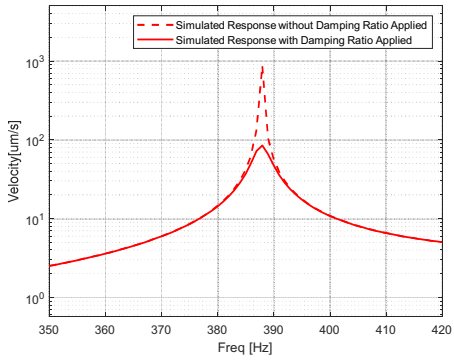

Fig. 9. Simulated PCB vibration velocity comparison for the case with and without damping ratio applied for mode 1 at the observation point.

The PCB model now is ready to simulate the harmonic response with an external force loaded. The board vibration velocity frequency response comparison for the measurement with force from the real coil and magnet system and the simulation with force from the simulated coil and magnet is given in Fig. 10. With the correctly set PCB material properties, damping ratio, and external loaded force, the frequency responses match well. The PCB vibration velocity is 35.49 μm/s from the measurement, and 35.75 μm/s from the simulation.

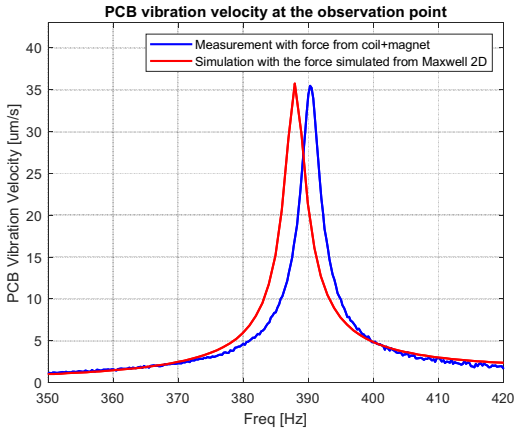

Fig. 10. PCB frequency response comparison

The PCB 1st resonance mode pattern comparison between the measurement and the simulation is given in Fig. 11. The patterns of PCB 1st resonance mode also have a good correlation.

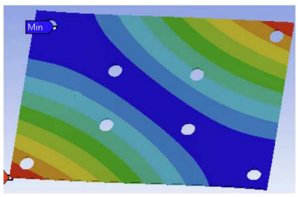

(a)

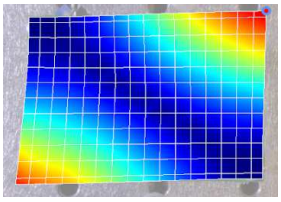

(b)

Fig. 11. PCB resonance mode pattern comparison (a) from simulation, (b) from measurement.

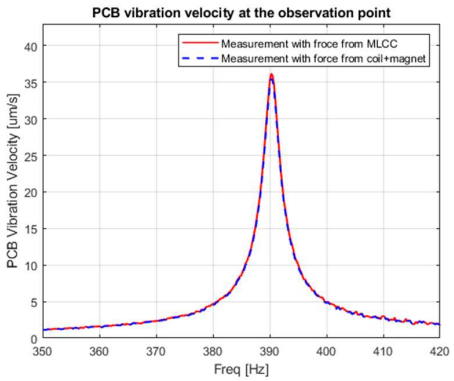

Fig. 12. PCB vibration velocity at mode 1 when the force is from MLCC and from the equivalent force.

Since the observation frequency is within a small range, the capacitor vibration-generated force can be assumed as a constant. The electromagnetic force generated from the coil-magnet system is also a constant, which is consistent with the assumption. Moreover, the equality of the electromagnetic force and the MLCC force can be justified by the PCB vibration velocity response level. For the example in [11], when the MLCC is soldered at the location short edge center of the PCB and is excited with a 1V DC plus 0.4Vpp AC voltage, the PCB vibration velocity response at the observation point is shown in Fig. 12 and the vibration velocity is 36.2 $\mu m/s$ at the mode frequency. The force from the coil-magnet system caused PCB vibration is 35.49 $\mu m/s$ as shown in Fig. 10, which has a good equivalence to the force from the capacitor. It shows that when giving the nominal electrical input to the MLCC, the capacitor vibration-caused PCB vibration is also at the microns per second. So the force of cap vibration should also be at the level of micron Newton.

Good consistency of the two forces is shown. By controlling the input current to the coil and changing the coil and magnet dimensions and positions, a force with the same magnitude as that from the MLCC can be generated.

V. Conclusions

In this paper, a small and controllable force is found to mimic the on-PCB MLCC vibration-induced force on the system. The equivalent force is the electromagnetic force between the coil and the magnet system. The behavior of the equivalent force is well-matched with the real system response when MLCC is excited.

Having a knowable force is good for the electronics in the simulation and prediction of the system response. Based on the process of finding the equivalent force proposed in this paper, more work can be done to make the analysis of electronic products in the Multiphysics domain much more complete, for example, investigating the methodology of obtaining the force from on-PCB electrical component directly, extracting the real force generated by the MLCC vibration, establishing the MLCC electrical input mechanical output transfer function, and have the sound level prediction.

References

[1] J. Kim, Y. Takita, K. Araki and J. Fan, "Improved target impedance for power distribution network design with power traces based on rigorous transient analysis in a handheld device," *IEEE Transactions on Components, Packaging and Manufacturing Technology*, vol. 3, no. 9, pp. 1554-1563, Sept. 2013.

[2] B. Zhao et al., "Decoupling capacitor power ground via layout analysis for multi-layered PCB PDNs," in *IEEE Electromagnetic Compatibility Magazine*, vol. 9, no. 3, pp. 84-94, 3rd Quarter 2020, doi: 10.1109/MEMC.2020.9241560.

[3] T. L. Jordan and Z. Ounaies, "Piezoelectric ceramics characterization," *Nat. Aeronaut. Space Admin. (NASA)*, WA, USA ICASE Rep. 2001-28, Sep. 2001.

[4] Y. Sun, S. Wu, J. Zhang, C. Hwang and Z. Yang, "Simulation Methodologies for Acoustic Noise Induced by Multilayer Ceramic Capacitors of Power Distribution Network in Mobile Systems," in *IEEE Transactions on Electromagnetic Compatibility*, vol. 63, no. 2, pp. 589-597, April 2021, doi: 10.1109/TEMC.2020.3019438.

[5] X. Yan, S. Wu, M. Xue, C. K. B. Leung, D. Beetner and J. Zhang, "A Practical Simulation Flow for Singing Capacitor Based Acoustic Noise Analysis," *2022 IEEE International Symposium on Electromagnetic Compatibility & Signal/Power Integrity (EMCSI)*, 2022, pp. 29-33, doi: 10.1109/EMCSI39492.2022.9889341.

[6] Y. Sun, S. Wu, J. Zhang, C. Hwang and Z. Yang, "Measurement Methodologies for Acoustic Noise Induced by Multilayer Ceramic Capacitors of Power Distribution Network in Mobile Systems," in *IEEE Transactions on Electromagnetic Compatibility*, vol. 62, no. 4, pp. 1515-1523, Aug. 2020, doi: 10.1109/TEMC.2020.2993850.

[7] H. Baek, D. Yu, J. Lee, H. Shim and J. -H. Kim, "Electrical approach to acoustic noise for MLCCs of power delivery network in mobile system," *2015 IEEE Electrical Design of Advanced Packaging and Systems Symposium (EDAPS)*, 2015, pp. 62-66, doi: 10.1109/EDAPS.2015.7383668.

[8] Ko, BH., Jeong, SG., Ahn, YG. et al. Analysis of the correlation between acoustic noise and vibration generated by a multi-layer ceramic capacitor. *Microsyst Technol 20*, 1671–1677 (2014). https://doi.org/10.1007/s00542-014-2209-5.

[9] S. -J. Chen, J. -L. Huang, G. -J. Wu, C. -L. Wu and S. -S. Pan, "Design and characterization of a PCB based capacitive shear force sensor for robotic gripper application," *2013 Seventh International Conference on Sensing Technology (ICST)*, 2013, pp. 884-888, doi: 10.1109/ICSensT.2013.6727777.

[10] K. -R. Lin, C. -H. Chiang, C. -H. Chang and C. -H. Lin, "Development of a novel force sensor system built with an industrial multilayer ceramic capacitor (MLCC)," *2012 7th IEEE International Conference on Nano/Micro Engineered and Molecular Systems (NEMS)*, 2012, pp. 487-490, doi: 10.1109/NEMS.2012.6196823.

[11] Y. Ding, J. Zhang, M. Xue, X. Hua, B. Leung, E. A. MacIntosh, and C. Hwang, "Extraction for Multilayer Ceramic Capacitor Vibration Induced Force", *2023 IEEE International Symposium on Electromagnetic Compatibility, Signal & Power Integrity (EMC+SIPI)*, accepted.